

Commensurate Spin Dynamics in the Superconducting State of an Electron-Doped Cuprate Superconductor

K. Yamada,^{1,*} K. Kurahashi,^{2,†} T. Uefuji,¹ M. Fujita,¹ S. Park,^{3,4} S.-H. Lee,³ and Y. Endoh⁵

¹*Institute for Chemical Research, Kyoto University, Uji 611-0011, Japan*

²*Department of Physics, Tohoku University, Aramaki Aoba, Sendai 980-8577, Japan*

³*NIST Center for Neutron Research, National Institute of Standards and Technology, Gaithersburg, Maryland 20899-8652*

⁴*Department of Materials and Nuclear Engineering, University of Maryland, College Park, Maryland 20742*

⁵*Institute of Materials Research, Tohoku University, Sendai 980-8577, Japan*

(Received 29 October 2002; published 4 April 2003)

We report neutron scattering studies on two single crystal samples of the electron-doped (*n*-type) superconducting (SC) cuprate $\text{Nd}_{2-x}\text{Ce}_x\text{CuO}_4$ ($x = 0.15$) with $T_c = 18$ and 25 K. Unlike the hole-doped (*p*-type) SC cuprates, where *incommensurate* magnetic fluctuations commonly exist, the *n*-type cuprate shows *commensurate* magnetic fluctuations at the tetragonal $(1/2\ 1/2\ 0)$ reciprocal points both in the SC and in the normal state. A spin gap opens up when the *n*-type cuprate becomes SC, as in the optimally doped *p*-type $\text{La}_{2-x}\text{Sr}_x\text{CuO}_4$. The gap energy, however, increases gradually up to about 4 meV as T decreases from T_c to 2 K, which contrasts with the spin pseudogap behavior with a T -independent gap energy in the SC state of *p*-type cuprates.

DOI: 10.1103/PhysRevLett.90.137004

PACS numbers: 74.25.Ha, 74.72.Jt

High- T_c superconductivity emerges when charge carriers, holes, or electrons are doped into an antiferromagnetic (AF) Mott insulator [1–3]. The mechanism of the superconductivity lies on their common two-dimensional CuO_2 planes into which the charge carriers go. One of the issues in understanding the mechanism is the question of the electron-hole symmetry. The electronic structure of the optimally doped cuprates shows evidence for the electron-hole symmetry [4,5]. Their phase diagrams as a function of doping, however, are asymmetric [6]. For hole doping, antiferromagnetism rapidly weakens and is replaced by a spin-glass-like phase with characteristics of incommensurate spin correlations and pseudogap in transport measurements. The pseudogap temperature, T^* , is well defined in the underdoped region and decreases with doping. The system becomes superconducting (SC) over a wide range of the hole concentration, x , around the optimal $x = 0.15$. The SC state has incommensurate spin correlations with a T -independent spin gap. The normal state of the underdoped and optimally doped SC region also shows unusual non-Fermi-liquid (FL) behaviors. There is increasing evidence for a quantum critical point (QCP) around the optimal doping which is responsible for the unusual properties of the SC and the normal phase [7–10]. For the electron-doped (*n*-type) cuprates, on the other hand, antiferromagnetism survives until the superconductivity appears over a narrow range of x around the optimal $x \sim 0.15$. The normal state of the *n*-type cuprates shows Fermi-liquid T^2 behavior in resistivity rather than the linear behavior of the hole-doped (*p*-type) cuprates. Therefore, investigating similarities and differences of the *n*-type and *p*-type cuprates would be crucial to understanding physics of the high- T_c superconductivity.

In this paper, we report neutron scattering measurements on single crystals of the *n*-type SC cuprate $\text{Nd}_{2-x}\text{Ce}_x\text{CuO}_4$ (NCCO) ($x = 0.15$) with $T_c = 18$ and 25 K. We have found *commensurate* magnetic fluctuations at the tetragonal $(1/2\ 1/2\ 0)$ reciprocal points in the SC and normal states. A spin gap opens up when the system becomes SC, as in the optimally doped *p*-type $\text{La}_{2-x}\text{Sr}_x\text{CuO}_4$ [11–13]. The gap energy, however, increases gradually up to about 4 meV as T decreases from T_c to 2 K, which contrasts with the T -independent spin pseudogap energy for the SC state of the *p*-type cuprate near T_c . Our results indicate that doped electrons self-organize in a different way than holes that form stripes such as in $(\text{La}, \text{Nd})_{2-x}\text{Sr}_x\text{CuO}_4$ [14,15], $\text{La}_{2-x}(\text{Sr}, \text{Ba})_x\text{CuO}_4$ [16], and the isostructural insulator $\text{La}_{2-x}\text{Sr}_x\text{NiO}_4$ [17,18].

Sizable single crystals of NCCO with $x = 0.15$ were grown by a traveling-solvent-floating-zone (TSFZ) method. The as-grown crystal is an AF insulator with the Néel temperature T_N of around 125 to 160 K depending on the excess oxygen concentration in the crystal. Bulk superconductivity appears only with proper heat treatments on these as-grown crystals. The detailed procedure of the crystal growth and the heat treatment is described in a separate paper [19]. For the SC sample, T_c is determined from zero-field-cooled diamagnetic susceptibilities measured by a SQUID magnetometer. For the present study, we used two SC samples with $T_c = 18$ and 25 K. SC transition temperature width is ~ 3 K and ~ 5 K for samples with $T_c = 18$ and 25 K, respectively. An almost full Meissner fraction was obtained in both samples [19].

Neutron scattering experiments were performed on the thermal neutron triple-axis spectrometer of Tohoku

University, TOPAN, and the cold neutron triple-axis spectrometer of the University of Tokyo, HER, installed at JRR-3M in JAERI, Tokai Establishment. We performed the experiment with low energy excitations below 1 meV on the cold neutron triple-axis spectrometer, SPINS, at the National Institute of Standards and Technology (NIST) Center for Neutron Research. Incident neutron energies of 13.7 meV for TOPAN and 5 meV for HER and SPINS were selected using the (0 0 2) reflection of pyrolytic graphite monochromators. Additionally, in order to eliminate the higher-order reflected beams, a pyrolytic graphite filter for thermal neutrons and a Be filter for cold neutrons were placed in the up or down stream of the sample position. Previously, a few attempts have been made to study spin dynamics in NCCO using a neutron scattering technique [20]. However, no well-defined magnetic signal has been found in the SC phase. In the previous measurements, the total volume of the sample was 0.5 cm^3 and the $(h h l)$ scattering plane was examined. For our study, we have investigated mostly the $(h k 0)$ scattering plane to increase the signal from two-dimensional magnetic rod along the c axis by using the larger vertical angular divergence of the beam. Furthermore, we cut a long single crystalline rod with a total volume of 2 cm^3 into three pieces and stacked those vertically using an aluminum sample holder. The holder was mounted in an aluminum can attached either to the cold plate of a ^4He -closed cycle refrigerator, or to a top-loading liquid-He cryostat, which cools down to 1.5 K.

Figure 1(a) shows temperature dependence of elastic neutron scattering intensity at $(3/2 \ 1/2 \ 0)$ reflection, obtained from three samples: the as-grown insulating sample and the two heat-treated SC samples with $T_c = 18$ and 25 K. For the as-grown insulating sample, upon cooling the intensity starts gradually increasing below $T_N \sim 140$ K, signaling the AF long range order of Cu^{2+} moments. It further increases below $T_{\text{Nd}} \sim 20$ K due to the participation of Nd^{3+} moments. When the sample gets the proper heat treatment and becomes SC, the static magnetic order is drastically suppressed. Even though the magnetic elastic peaks remain even in the SC phase, the SC samples have lower $T_N \sim 60$ to 80 K and T_{Nd} , and weaker intensity than the insulating sample. The suppression is more severe for the SC sample with the higher $T_c = 25$ K than for the one with $T_c = 18$ K. The width of the static peak was resolution limited for the insulating sample and was broadened for the SC samples. By fitting the static peak with a Lorentzian convoluted with the instrumental resolution, we obtained the in-plane and the out-of-plane correlation length, $\xi_{ab} = 150(60) \text{ \AA}$ and $\xi_c = 80(30) \text{ \AA}$, respectively, at $T = 8$ K for the $T_c = 25$ K sample. This indicates that superconductivity competes with the magnetic order in the n -type cuprate as in p -type cuprates.

To investigate the relationship between the superconductivity and the dynamic spin correlations, we have

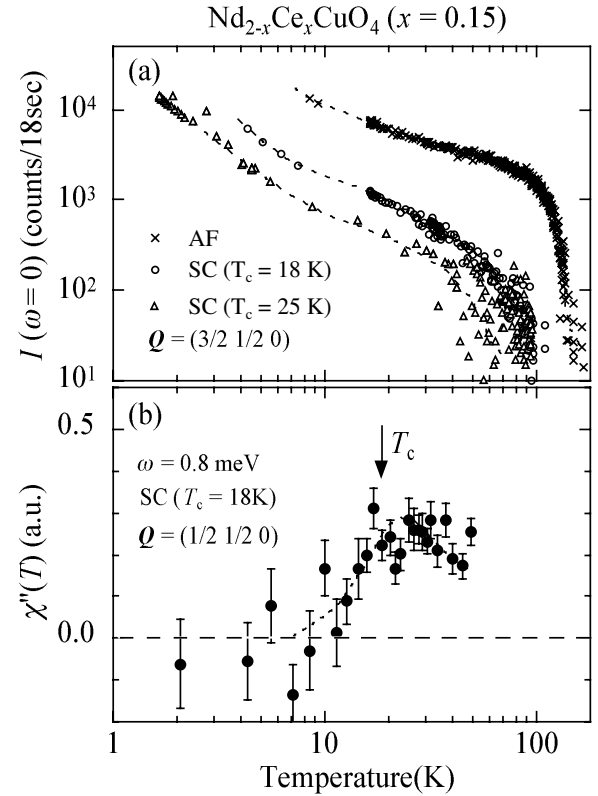


FIG. 1. (a) T dependence of the elastic magnetic peak intensities of NCCO ($x = 0.15$) at $(3/2 \ 1/2 \ 0)$ measured from an as-grown insulating (crosses) and the two reduced SC single crystals with $T_c = 18$ K (open circles) and 25 K (open triangles). (b) T dependence of dynamical susceptibility $\chi''(\omega = 0.8 \text{ meV})$ at $(1/2 \ 1/2 \ 0)$ obtained from the reduced sample of NCCO ($x = 0.15$, $T_c = 18$ K). Dotted curves are to guide the eye.

performed constant energy scans around the AF $(1/2 \ 1/2 \ 0)$ point. Figure 2(a) shows the results for the normal state obtained with $\omega = 2$ meV, with scans along the $[1 \ 0 \ 0]$ and $[1 \ 1 \ 0]$ directions, which are parallel and diagonal to Cu-O bonds in the CuO_2 plane, respectively. In both directions, a commensurate peak appears. These results sharply contrast with the incommensurate peaks found in the p -type SC cuprates [14]. Solid lines are the best fits to a Gaussian convoluted with the instrumental resolution function yielding the intrinsic half width at half maximum (HWHM) of $0.025(3)a^*$. Indeed, the data shown in Fig. 2(a) are the first direct experimental evidence for the commensurate spin fluctuations in the n -type cuprate. The peak widths of the SC samples are substantially broader than those of the AF phase, while the q -integrated peak intensities are comparable between the AF and SC samples except at low temperatures below T_c . Furthermore, the peak width is broader for the $T_c = 25$ K sample than the $T_c = 18$ K sample. Figure 1(b) shows that for $\omega = 0.8$ meV the commensurate spin fluctuations diminish as T decreases below T_c , which indicates opening of a spin gap in the SC state.

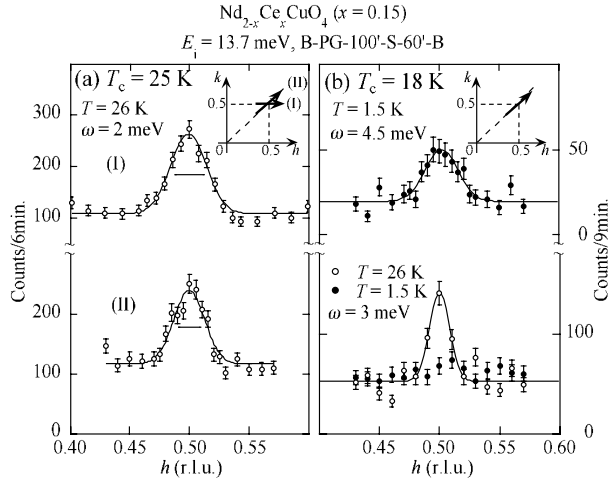


FIG. 2. Constant- ω scans around $(1/2\ 1/2\ 0)$ obtained from two reduced samples of NCCO [$x = 0.15$]; (a) $T_c = 25$ K and (b) $T_c = 18$ K] in the normal ($T = 26$ K, open circles) and SC ($T = 1.5$ K, closed circles) phases. (a) (upper) 26 K, normal, $\omega = 2$ meV, with scans along the $(h\ 0\ 0)$ direction and (lower) 26 K, normal, $\omega = 2$ meV, with scans along the $(h\ h\ 0)$ direction. (b) (upper) 1.5 K, SC, $\omega = 4.5$ meV, with scans along the $(h\ h\ 0)$ direction and (lower) 26 K, normal and 1.5 K, SC, $\omega = 3$ meV, with scans along the $(h\ h\ 0)$ direction. Horizontal bars indicate the full width at half maximum of the instrumental resolution. Solid curves are explained in the text.

Figure 2(b) clearly shows the depletion of the spectral weight for $\omega \leq 3$ meV. To study energy dependence of the dynamic spin fluctuations in detail, we have performed constant ω scans shown in Fig. 2 with various energy transfers. The data were fitted to a Gaussian convoluted with the instrumental resolution function. The integrated intensity of the Gaussian was converted to the imaginary part of dynamic susceptibility via the fluctuation dissipation theorem, $I(\omega) \propto \chi''(\omega)[1 + n(\omega)]/\pi$, where $n(\omega)$ is the Bose thermal population factor. Figure 3 shows the resulting $\chi''(\omega)$ as a function of the energy transfer, ω . For both SC samples, at $T = 2$ K, $\chi''(\omega)$ has a gap of $2\Delta \sim 3$ meV and 4 meV for the $T_c = 18$ and 25 K samples, respectively. The fact that the sample with the higher T_c has the larger 2Δ , whereas it has the weaker Nd ordering and the lower T_{Nd} , tells us that the gapped commensurate spin fluctuation is an intrinsic property of the spin dynamics in the optimally doped n -type superconductor. Such a spin gap has also been reported in the p -type $\text{La}_{2-x}\text{Sr}_x\text{CuO}_4$ near optimal doping. A spin gap of $2\Delta = 6 \sim 7$ meV was observed in the optimally doped $\text{La}_{2-x}\text{Sr}_x\text{CuO}_4$ [12,13]. As shown in the inset of Fig. 4, their maximum gaps $2\Delta_{\max}$ behave linearly with the SC temperature scale $Ck_B T_c$ with $C = 2.0(2)$, irrespective of carrier type. There is, however, a qualitative difference of the spin dynamics between the n -type and the p -type cuprates: For the n -type $\text{Nd}_{2-x}\text{Ce}_x\text{CuO}_4$ ($x = 0.15$), as shown in Fig. 3, upon warming $\chi''(\mathbf{Q}, \omega)$ shifts toward lower energies and

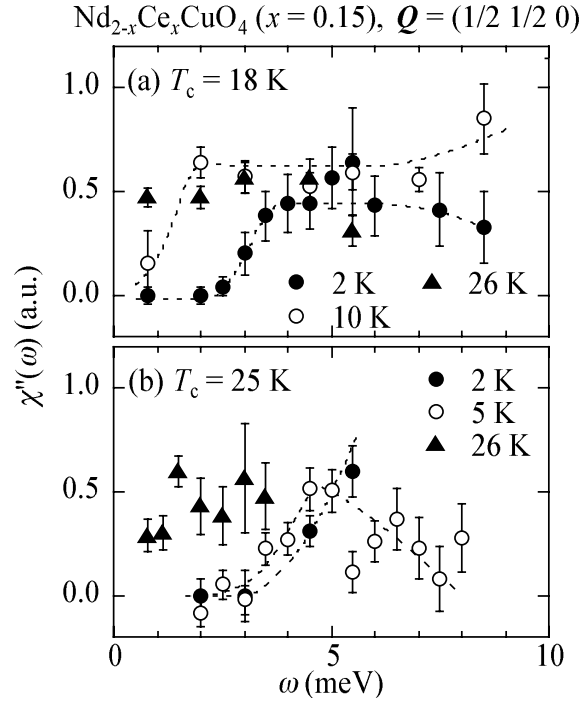


FIG. 3. Energy spectra of $\chi''(\omega)$ obtained from the normal and SC phases (a) of NCCO ($x = 0.15$, $T_c = 18$ K) and (b) of NCCO ($x = 0.15$, $T_c = 25$ K). Dotted curves are to guide the eye.

eventually fills up the gap in the normal phase. The shift of the spectral weight in the energy spectrum is summarized in Fig. 4: 2Δ decreases with increasing T and eventually disappears when the system enters the normal phase. This suggests the absence or degradation of a spin pseudogap state and is in sharp contrast with those observed in the $\text{La}_{2-x}\text{Sr}_x\text{CuO}_4$ ($x = 0.15$) in which, for $T \ll T_c$, $\chi''(\mathbf{Q}, \omega)$ diminishes for all $\omega < 2\Delta$, and as T approaches T_c , $\chi''(\mathbf{Q}, \omega)$ smears into lower ω without remarkable change in 2Δ [11,12]. Recent NMR measurements on single crystalline n -type superconductor $\text{Pr}_{1-x}\text{LaCe}_x\text{CuO}_4$ also suggested the absence of spin pseudogap [21].

Commensurate short range spin correlations in the SC phase of the n -type cuprate suggest that the doped electrons may be inhomogeneously distributed or form droplets/bubbles in the CuO_2 planes, rather than organizing into one-dimensional stripes as the doped holes seem to do in the p -type cuprates. Their different orbital characters might be responsible for the different behaviors. Doped holes are dominantly introduced into the $2p_{xy}$ orbital of oxygen ions in CuO_2 planes and induce the frustrated magnetic interactions between the neighboring Cu spins which stabilize the formation of stripes. The elastic incommensurate magnetic signal increases when an external magnetic field is applied perpendicular to the CuO_2 planes [22–24]. On the other hand, doped electrons predominantly enter into the $3d_{x^2-y^2}$ orbitals of Cu ions to

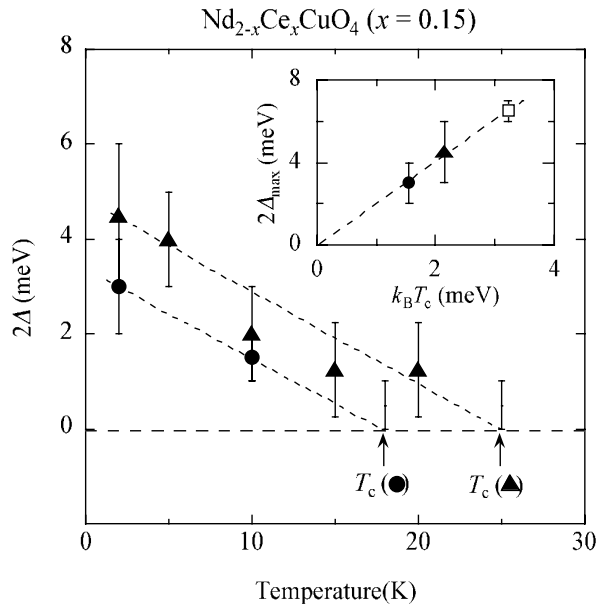


FIG. 4. T dependence of the spin gap, 2Δ for the n -type SC cuprate NCCO ($x = 0.15$) with $T_c = 18$ K (filled circles) and 25 K (filled triangles). Dotted lines are guides to the eye. At T_c , the spin gap is absent for both NCCO samples. The inset shows $2\Delta_{\text{max}}$ versus $k_B T_c$ obtained from our samples and LSCO ($x = 0.15$) (open square, data taken from Ref. [12]).

make the Cu site nonmagnetic, which reduces the size of the AF domains without introducing frustration or changing the commensurability. For the p -type SC cuprates, the quasi-two-dimensional stripe phase (or the pseudogap phase) competes with the SC phase, whereas for the n -type SC cuprates it is the three-dimensional AF state that competes with the superconductivity. Our results show that for n -type cuprates the antiferromagnetism coexists with superconductivity at the optimal region. This may indicate that the transition from the antiferromagnetism to superconductivity upon doping is a first order in nature and therefore it lacks a QCP. This difference may be responsible for their different properties in SC and normal states [25–27].

In summary, we revealed by a neutron scattering study on the single crystals of $\text{Nd}_{1.85}\text{Ce}_{0.15}\text{CuO}_4$ the coexistence of gapped commensurate spin fluctuations with the electron-doped superconductivity. The energy gap of around 4 meV closes at or near T_c , which suggests the absence or degradation of the spin pseudogap state in the electron-doped superconductor. A more comprehensive study on the electron-doped superconductor free from the effect of rare-earth magnetic moments is highly required for the full understanding of the universal properties of spin fluctuations irrespective of types of carrier.

We thank Y. Kojima, I. Tanaka, S. Hosoya, K. Hirota, H. Y. Kee, J. M. Tranquada, P. A. Lee, G. Shirane, and R. J. Birgeneau for their valuable discussions. This work was supported by the Japanese Ministry of Education, Culture, Sports, Science and Technology, Grant-in-Aid for Scientific Research on Priority Areas Contract, Scientific Research (A) and (B), Encouragement of Young Scientists, Creative Scientific Research, the Japan Science and Technology Corporation, the Core Research for Evolutional Science and Technology Project (CREST), and the National Science Foundation under Agreement No. DMR-9986442.

*Present address: yamada@scl.kyoto-u.ac.jp

†Present address: Kohzu Precision Co. Ltd., Setagaya, Tokyo 154-0005, Japan.

- [1] J. G. Bednorz and K. A. Müller, *Z. Phys. B* **64**, 189 (1986).
- [2] M. A. Kastner, R. J. Birgeneau, G. Shirane, and Y. Endoh, *Rev. Mod. Phys.* **70**, 897 (1998), and references therein.
- [3] Y. Tokura, H. Takagi, and S. Uchida, *Nature (London)* **337**, 345 (1989); H. Takagi, S. Uchida, and Y. Tokura, *Phys. Rev. Lett.* **62**, 1197 (1989).
- [4] T. Sato, T. Kamiyama, T. Takahashi, K. Kurahashi, and K. Yamada, *Science* **291**, 1517 (2001).
- [5] N. P. Armitage *et al.*, *Phys. Rev. Lett.* **86**, 1126 (2001); *Phys. Rev. Lett.* **87**, 147003 (2001); cond-mat/0201119.
- [6] A. Damascelli, D. H. Lu, and Z.-X. Shen, *J. Electron Spectrosc. Relat. Phenom.* **117–118**, 165 (2001), and references therein.
- [7] J. L. Tallon *et al.*, *Phys. Status Solidi (b)* **215**, 531 (1999).
- [8] J. L. Tallon and J. W. Loram, *Physica (Amsterdam)* **C349**, 53 (2001).
- [9] C. Kusko *et al.*, cond-mat/0201117.
- [10] C. Panagopoulos *et al.*, cond-mat/0007158.
- [11] K. Yamada *et al.*, *Phys. Rev. Lett.* **75**, 1626 (1995).
- [12] C.-H. Lee *et al.*, *J. Phys. Soc. Jpn.* **69**, 1170 (2000).
- [13] B. Lake *et al.*, *Nature (London)* **400**, 43 (1999).
- [14] J. M. Tranquada *et al.*, *Nature (London)* **375**, 561 (1995).
- [15] X. J. Zhou *et al.*, *Science* **286**, 268 (1999).
- [16] M. Fujita *et al.*, *Phys. Rev. Lett.* **88**, 167008 (2002).
- [17] J. M. Tranquada *et al.*, *Phys. Rev. Lett.* **79**, 2133 (1997).
- [18] S.-H. Lee *et al.*, *Phys. Rev. B* **63**, 060405 (2001).
- [19] K. Kurahashi *et al.*, *J. Phys. Soc. Jpn.* **71**, 910 (2002).
- [20] M. Matsuda *et al.*, *Phys. Rev. B* **45**, 12548 (1992).
- [21] G.-q. Zheng *et al.*, cond-mat/0211400.
- [22] S. Katano *et al.*, *Phys. Rev. B* **62**, R14677 (2000).
- [23] B. Lake *et al.*, *Nature (London)* **415**, 299 (2002).
- [24] B. Khaykovich *et al.*, *Phys. Rev. B* **66**, 014528 (2002).
- [25] S. Sachdev, *Science* **288**, 475 (2000).
- [26] C. M. Varma *et al.*, *Phys. Rep.* **361**, 267 (2002).
- [27] P. Coleman *et al.*, *J. Phys. Condens. Matter* **13**, R723 (2001).